

# Damping Factor of Composite Plate Using Lamb Wave Method

B A Ben, B S Ben, K. Adarsha Kumar, B S N Murthy

*Abstract- The article presents the methodology for finding material damping capacity at higher frequency and lower amplitudes. Lamb wave dispersion theory is used for finding the damping capacity of composite material which is used at extensively high frequency applications. The method has been implemented on carbon fiber reinforced polymer (CFRP) and glass fiber reinforced polymer (GFRP) plates. The Lamb waves or stress waves are generated using ultrasonic pulse generator with scan view plus as virtual controller and also calibration was carried out for optimal Lamb wave generation. The method is well explored in this article and the results have been compared with other conventional methods. The results were close agreement with the other methods used in this article.*

## I. INTRODUCTION

The damping capacity of a material is the fundamental property for designing and manufacturing structural components in dynamic applications. Materials with high damping capacity are very desirable to suppress mechanical vibration and transition of waves, thus decreasing noise and maintaining the stability of structural systems. Experimental and analytical characterization of damping is not easy, even with conventional structural materials, and the anisotropic nature of composite materials makes it even more difficult. Experimental approaches range from laboratory bench-top methods to portable field inspection techniques, whereas analytical techniques vary from simple mechanics-of-materials methods to sophisticated three-dimensional finite-element approaches. This article presents a Lamb wave method for finding damping capacity of a material using ultrasonic pulse generator experimental setup. Damping in composites involves a variety of energy dissipation mechanisms that depend on vibrational parameters such as frequency and amplitude and these are studied with nondestructive evaluation. In fiber-reinforced polymers, the most important damping mechanisms have been studied by Y. Chen and R. F. Gibson [1]. The nondestructive evaluation (NDE) techniques such as radiography, acoustic emission, thermal NDE methods, optical methods, vibration damping techniques, corona discharge and chemical spectroscopy, have also been applied to characterize the fiber-reinforced composites [2, 3]. Among these techniques, the vibration damping method, which is based on energy dissipation theory, has been increasingly used for measuring damping capacity. The principle of the method is based on the theory of energy dissipation. According to the theory, quality of interfacial adhesion in composites can be evaluated by measuring the part of energy dissipation contributed by the interfaces, assuming that the interface part can be obtained by separating those of matrix and fiber from the total composites. The energy dissipation of a

material can be evaluated by the damping of the material. Nowick and Berry summarized the techniques currently used for measuring vibration damping of materials and structures [4]. The techniques for the measurement of damping often deal with natural frequency or resonant frequency of a system. In general, all apparatus for the investigation of vibration can be categorized as free vibration (or free decay) and forced vibration. Free vibration is executed by a system in the absence of any external input except the initial condition inputs of displacement and velocity [5]. For example, it is possible to have a wire sample gripped at the top, and have a large weight hanging freely at the bottom; this system can be set either into longitudinal or torsional oscillation. The latter represents the well-known "torsion pendulum", developed by Ting-Sui K, in which the strain at any point can be expressed in terms of the angular twist of the inertia member. For a forced vibration, a periodic exciting force is applied to the mass. When the resonant frequency is achieved, the loss angle is obtainable directly from the width of the resonance peak at half-maximum in a plot of (amplitude) versus frequency. Typical forced vibration techniques include the free-free beam technique [6] and the piezoelectric ultrasonic composite oscillator technique (PUCOT) [7-9]. These techniques have been applied to dynamic mechanical analysis (DMA) which is a widely used technique in polymer studies, and has attracted even more attention for interface characterization. However, the instrument is relatively expensive and cannot be operated at a high frequency which can reflect more information from the tested materials. The damping of fiber reinforced composite materials has been studied extensively [10-12]. All of the published results for continuous fiber reinforced composites show that when strain levels are low the damping characteristics do not depend on strain amplitude but are dependent on fiber orientation, temperature, moisture absorption, frequency, and matrix properties. Fiber properties have only minimal effects. However, for discontinuous fiber reinforced composites it has been shown that the damping characteristics in the fiber direction are much greater than that obtained continuous fiber reinforced composites. It is commonly accepted that the main sources of damping in a composite material come from micro plastic or viscoelastic phenomena associated with the matrix and slippage at the interface between the matrix and the reinforcement.

Composite materials fall into two categories: fiber reinforced and particle (or whisker) reinforced composite materials. Both are widely used in advanced structures. Among the various kinds of composites, glass fiber-

reinforced polymer (GFRP) and carbon fiber-reinforced polymer (CFRP) composites have become more and more important in engineering applications because of their low cost, light weight, high specific strength and good corrosion resistance. This paper will emphasize viscoelastic damping, which appears to be the dominant mechanism in undamaged polymer composites vibrating at small amplitudes. An ultrasonic based Lamb wave method was developed to measure the damping capacity of composite material and the result has been validated with conventional DMA instrumentation.

## II. EXPERIMENTAL SETUP

### A. Ultrasonic Pulse Generator

The schematic diagram of the Ultrasonic pulse generator experimental setup is shown in fig. 1. The test specimen is clamped at one end on cantilever support fixed on basement and the transducers are placed on the test specimen at a distance of 160 mm from each other. A coupling fluid is used between transducers and the test specimen for getting good results. The Pitch-Catch RF Test Method, which uses a dual-element, point-contact, ultrasonic transducer has been used in which one element transmits a burst of acoustic waves into the test part, and a separate element receives the sound propagated across the test piece between the transducer tips, as shown in fig. 2. Both the actuation and the data acquisition are performed using a portable Panametrics-NDT™ EPOCH 4PLUS, and a desktop PC running Scan view plus as a virtual controller.

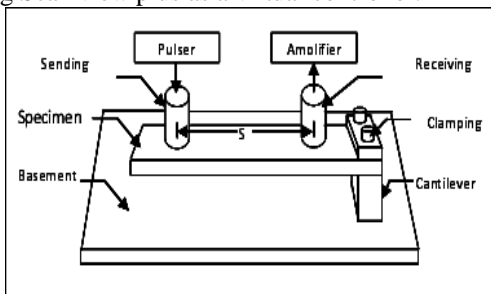


Fig. 1 Schematic Diagram of Experimental Setup



Fig. 2 Experimental Setup

Two panels of quasi-isotropic laminate of carbon fiber/epoxy (CFRP) and quasi-isotropic laminate of glass fiber/epoxy (GFRP) have been fabricated by the standard process and the specimens are cut to 250 x 50 x 2 mm using a continuous diamond grit cutting wheel.

### i. Calibration Of Ultrasonic Pulse Generator For Optimal Lamb Wave Generation

The Panametrics-NDT™ EPOCH 4PLUS is capable of producing ultrasonic sound waves and is equipped with four channels i.e. Device, Pulsar, Receiver and Waveform. Each channel is having editable parameters tabulated below.

Table 1. Parameters

Channels	Editable Parameters					
Device	Unit	Angle	Thickness			
Pulsar		Mode	Energy	Wave Type	Frequency	
Receiver		Gain	Broad band	Low pass	High pass	Bypass
Waveform		Range	Rectification	Offset		

The optimal driving frequency for different specimens is obtained by varying different editable parameters shown in the above table. Fig. 3 shows the calibration of ultrasonic pulse generator for CFRP specimen based on the fitted peak value and similarly it is calibrated for various materials. Curves have been plotted between pulser frequency and signal amplitude at receiver for different materials to find optimal driving frequency and it is shown in fig. 4. A Histogram representation of percentage amplitude of waveform at constant gain which is used to attain a trend line for optimal driving frequency for different materials is shown in fig. 8 and the % amplitude of the waveform at various pulser frequencies is taken as Bin range (0-820 kHz) at constant gain 55 (db) for different materials.

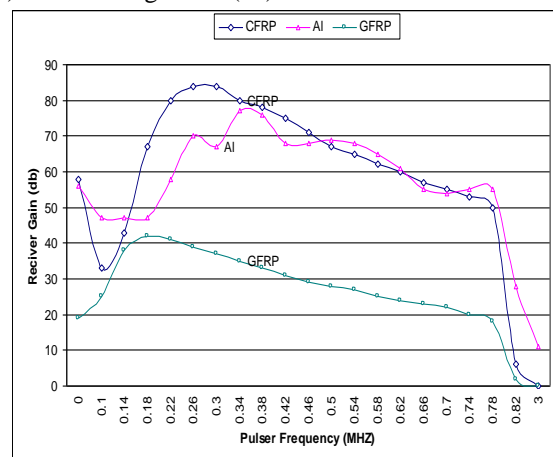


Fig. 3 Optimal Driving Frequency Selection for Different Materials

The frequency of the transducer to be used is proportional to the acoustic impedance of the layer. Materials such as graphite or fiberglass with low impedance require lower frequency transducers than metal skin layers. It is observed that the frequencies in the range of 100 KHz to 460 kHz have been useful in most of the testing. The higher frequencies are used for thinner and metallic layers

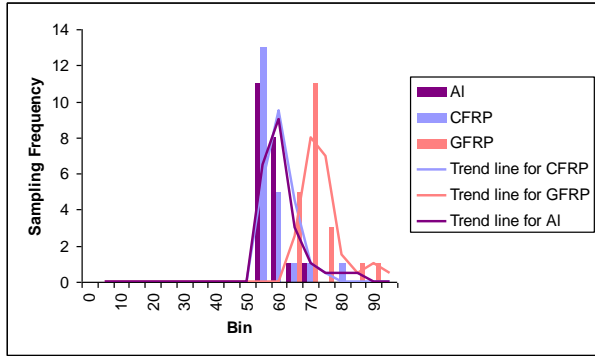


Fig. 4 Histogram Representation of % Amplitude of Waveform at Constant Gain

**B. Dynamic Mechanical Analyzer**

The schematic diagram of the GABO Eplexor Dynamic Mechanical Analyzer (DMA) is shown in (Fig. 3). Rectangular specimens (30mmx12mmx2mm) were prepared by using a continuous diamond grit cutting wheel for damping measurements. Tests were carried under a static load of 50N and a dynamic load of 40N at room temperature for the frequencies ranging from 1Hz to 25Hz using three- point bending testing mode. The damping capacity was determined by  $\tan \delta$ , where  $\delta$  was the lag angle between the applied strain and the response stress. The damping capacity ( $\tan \delta$ ) is calculated from the following relation.

$$\tan \delta = E''/E' \quad (1)$$

Where  $E'$  is the dynamic storage modulus and  $E''$  is loss modulus.

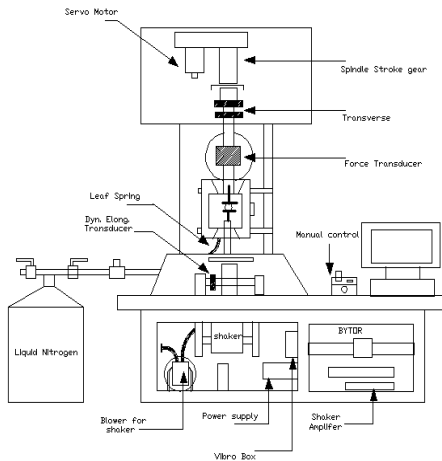


Fig 5 Schematic diagram of GABO Eplexor DMA

**III. LAMB WAVE DISPERSION THEORY**

There are two groups of Lamb waves, symmetric and anti-symmetric, that satisfy the wave equation and boundary conditions for this problem and each can propagate independently of the other. A graphical representation of these two groups of waves can be seen in Fig. 4. In the following section, analytical models for Lamb wave propagation have been derived, which relate the velocity of the wave-front to the actuating frequency.

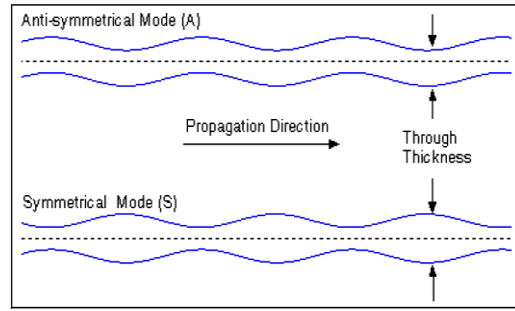


Fig. 6 Graphical Representation of A and S Lamb Wave Shapes

The most descriptive way to represent the propagation of a Lamb wave in a particular material is with their dispersion curves, which plot the phase and group velocities versus the excitation frequency [13]. The derivation of these curves begins with the solution to the wave equation for the anti-symmetric Lamb wave as seen in eq. 2:

$$\frac{\tanh \beta f}{\tanh \alpha f} = \frac{(\xi^2 + \beta^2)^2}{4\xi^2 \alpha \beta} \quad (2)$$

Where

$$\alpha = \sqrt{\xi^2 - h^2}, \quad \beta = \sqrt{\xi^2 - k^2}$$

$$h^2 = \frac{\rho \omega^2}{\lambda + 2\mu}, \quad k^2 = \frac{\rho \omega^2}{\mu}, \quad \xi^2 = \frac{\omega^2}{c_{phase}^2}, \quad f = \frac{t}{2}$$

$$\mu = \frac{E}{2(1+\nu)}, \quad \lambda = \frac{E\nu}{(1-2\nu)(1+\nu)}$$

The hyperbolic terms can be eliminated by using the identity

$$\tanh(iz) = i \tan(z)$$

$$\frac{\tanh \beta f}{\tanh \alpha f} = \frac{\tanh \sqrt{h^2 - \xi^2} f i}{\tanh \sqrt{k^2 - \xi^2} f i} = \frac{\tan \sqrt{h^2 - \xi^2} f}{\tan \sqrt{k^2 - \xi^2} f} \quad (3)$$

Substituting into both sides and collecting like terms the equation becomes:

$$\tan \sqrt{1 - \frac{\mu}{\rho c_{phase}^2}} \sqrt{\frac{\rho}{\mu}} \frac{\omega t}{2} = \frac{4 \frac{1}{c_{phase}^2} - 4 \frac{1}{\mu} + \frac{\rho^2}{\mu^2} c_{phase}^2}{4 \sqrt{1 - \frac{\rho}{\lambda + 2\mu}} \frac{c_{phase}^2}{\mu} \sqrt{1 - \frac{\rho}{\mu} c_{phase}^2}} \quad (4)$$

Now, by collecting the terms into the following non-dimensional parameters, the equation given in [11] is recovered (note that  $\xi$  is a different variable than the one used by Lamb)

$$\xi^2 = \frac{\mu}{(\lambda + 2\mu)}, \quad \zeta^2 = \frac{\mu}{\rho c_{phase}^2}, \quad \bar{d} = \frac{\omega t}{2} \sqrt{\frac{\rho}{\mu}} \quad (5)$$

$$\frac{\tan(\bar{d}\sqrt{1-\zeta^2})}{\tan(\bar{d}\sqrt{\xi^2-\zeta^2})} + \frac{(2\xi^2-1)^2}{4\xi^2\sqrt{1-\zeta^2}\sqrt{\xi^2-\zeta^2}} = 0 \quad (6)$$

where the non-dimensional parameters are

$$\xi^2 = \frac{c_i^2}{c_i^2}, \zeta^2 = \frac{c_i^2}{c_{phase}^2}, \bar{d} = \frac{k_i t}{2} \quad (7)$$

For an isotropic material, these parameters can be defined in terms of Lamé's constants:

$$\mu = \frac{E}{2(1+\nu)}, \lambda = \frac{E\nu}{(1-2\nu)(1+\nu)} \quad (8)$$

In which case:

$$c_i^2 = \frac{\mu}{\rho}, c_i^2 = \frac{(\lambda+2\mu)}{\rho}, k_i = \frac{\omega}{c_i} \quad (9)$$

Substituting these equalities into the non-dimensional parameters yields:

$$\xi^2 = \frac{\mu}{(\lambda+2\mu)} = \frac{1-2\nu}{2-2\nu}, \zeta^2 = \frac{\mu}{\rho c_{phase}^2} = \frac{E}{2\rho(1+\nu)c_{phase}^2} \quad (10)$$

$$\bar{d} = \frac{\omega t}{2c_i} = \frac{\omega t}{2} \sqrt{\frac{\rho}{\mu}} = \frac{\omega t}{2} \sqrt{\frac{2\rho(1+\nu)}{E}} \quad (11)$$

Finally, eq. (12) is substituted into eq. (7) and it is solved numerically in Mathematica<sup>TH</sup>. The equations presented are intended for isotropic materials; however it has been shown in the literature that the Ao mode is fairly invariant to the layup of a composite material, and can be closely approximated by using the bulk laminate properties [14]. For a given material, the Young's Module in the propagation direction as  $E$ , Poisson Ratio  $\nu$ , and the density  $\rho$  are known, and the phase velocity ( $c_{phase}$ ) is the dependent variable being solved for the independent variable being iteratively supplied is the frequency-thickness product, where  $\omega$  is the driving frequency in radians. The other useful plot is the group velocity dispersion curve, which can easily be derived from the phase velocity curve using eq. (13):

$$k = \frac{2\pi}{\lambda_w} (\text{wavenumber}), \lambda_w = \frac{c_{phase}}{f} (\text{wavelength}) \quad (12)$$

$$c_{group} = c_{phase} + \frac{\partial c_{phase}}{\partial k} k = \frac{c_{phase}}{1 - \frac{f}{c_{phase}} \frac{\partial c_{phase}}{\partial f}}$$

Where  $f$  is the frequency in Hz. At low frequencies, the Ao phase velocity can be approximated in the form of  $A\omega^{1/2}$  and the complementing group velocity as  $2A\omega^{1/2}$ , where  $A$  is a material property dependent constant. At higher frequencies

the phase velocity for this mode tends to the Rayleigh velocity:

$$c_R = \left( \frac{0.87 + 1.12\nu}{1 + \nu} \right) c_i \quad (13)$$

These dispersion curves are the key to describing and understanding the propagation of Lamb waves in a solid medium, and will be used in the following sections to find damping capacity of a material.

#### IV. METHODOLOGY

In the present work a methodology has been proposed for finding damping capacity of a material using Lamb wave propagation theory and its process flow diagram is shown in fig. 7 [4].

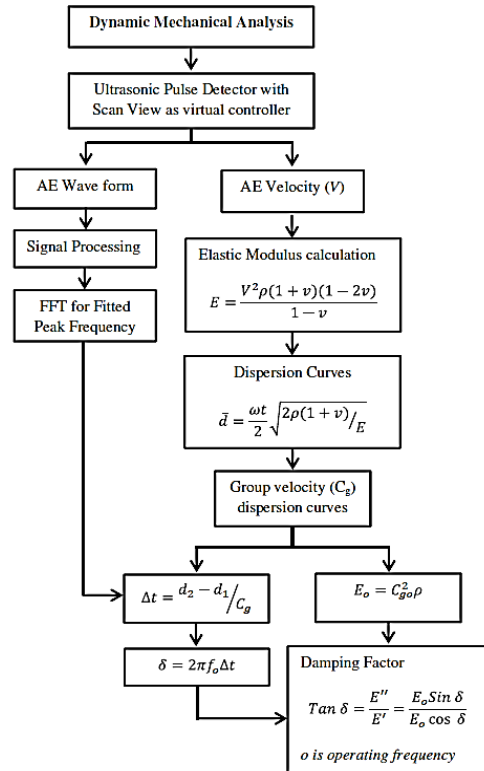


Fig. 7 Process Flow Diagram for Dynamic Mechanical Analysis by Lamb Waves

The relationship between the material properties of a specimen and the velocity of the propagating Lamb wave is quite complex, however an understanding is necessary to design an appropriate method for finding damping capacity of a material. In the Lamb wave equation the first order the wave velocity increases with the square root of the modulus, i.e. an increase in modulus slightly speeds the wave velocity. An increase in the density would have the opposite effect slowing wave velocity, as it appears in all the same terms as the modulus but on the reciprocal side of the divisor. The effect of the Poisson's ratio is probably the most complicated, as it appears in most of the terms, and small changes seem to have little to no effect on the wave velocity.

The basic material property Young’s modulus can be determined quickly and easily through computations based on Lamb wave velocities [15-17]. Young’s modulus is determined using the relation given below

$$E = \frac{V^2 \rho (1 + \nu)(1 - 2\nu)}{1 - \nu} \quad (14)$$

Where  $V$  is velocity of sound traveling in the material,  $\rho$  is material density and  $\nu$  is Poisson’s ratio. The velocities of the specimens are determined experimentally using ultrasonic pulse generator test setup and the Young’s modulus is calculated by using eq. (14) and thus obtained Young’s modulus is substituted in eq. (11) discussed in previous section for finding dispersion characteristics. The group velocity at fitted peak frequency and with known distance between probes ( $d_2 - d_1$ ),  $\Delta t$  is calculated. Thus obtained  $\Delta t$  is substituted in eq. (15) to determine the phase shift at fitted peak frequency or iteratively supplied frequency for finding material damping capacity ( $Tan \delta$ ). Dynamic mechanical analysis can be carried out using the same procedure by getting the  $E_0$  value from group velocity dispersion at iteratively supplied frequencies.

$$\delta = 2\pi f \Delta \quad (15)$$

### V. RESULTS AND DISCUSSION

Many researches carried damping measurements in temperature sweep mode but the present work involves frequency sweep since the damping is to eliminate the noise and vibrations resulting from frequency in many industrial applications. In the present work damping measurements were carried out using Lamb wave method and a GABO Eplexor Dynamic Mechanical Analyzer (DMA). The GFRP and CFRP plates have been tested in this work and their material properties are tabulated in table 1. The wave form from the instrument is processed through virtual controlling software to find the fitted peak frequency of the test specimens. The continuous waveform is subjected to fast Fourier transform (FFT) which yield a single peak from the calibrated optimal driving frequency, however for a few finite cycles, the FFT appears as a Gaussian curve with a peak at the driving frequency and it is shown in fig. 8.

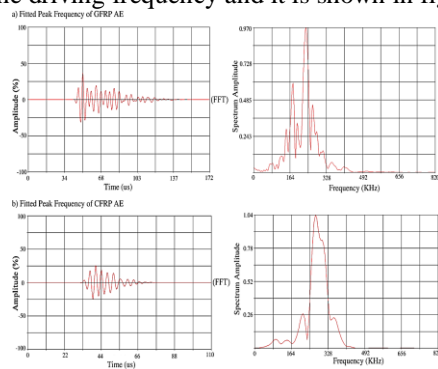


Fig. 8 Signal Processing Of the Continuous Wave Form  
A) GFRP Specimen B) CFRP Specimen

The phase and group velocity dispersion curve for the Lamb wave using the material properties from the specimens is used in the present research can be seen in fig. 9 and fig. 10. These Lamb wave dispersion curves have been obtained from the iterative supply of the frequency and this has been performed using Mathematica<sup>TH</sup> code. The group and phase velocities of the test specimens at their fitted peak frequency along with  $\Delta t$  have been shown in table 2. Using all the data derived in this section  $Tan \delta$  is calculated and also it has been compared with other methods for validation as shown in table 3.

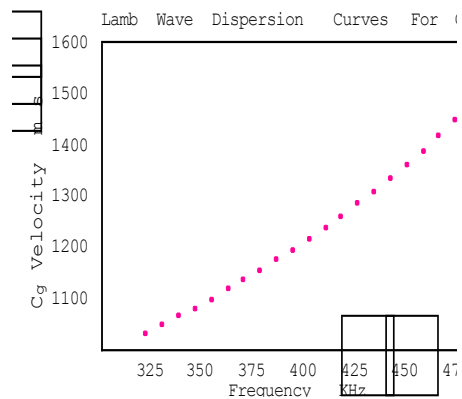


Fig. 9 Lamb Wave Dispersion Curves CFRP

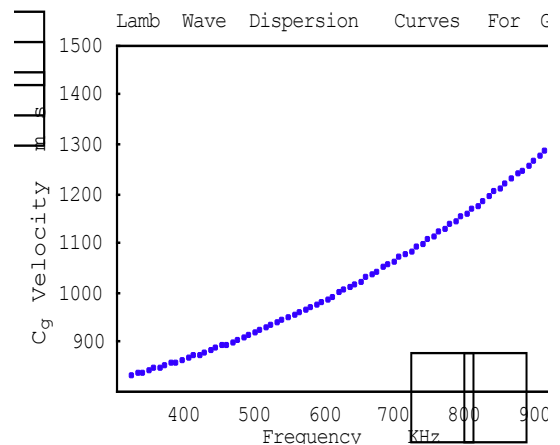


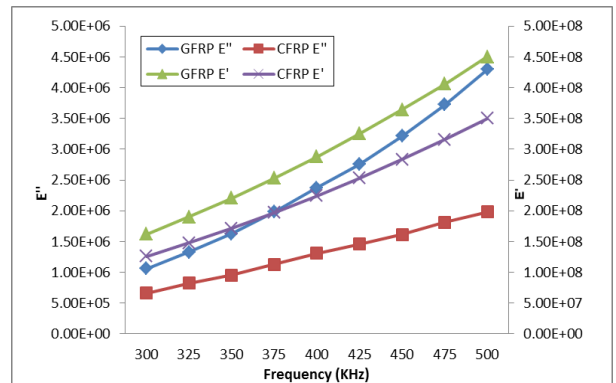
Fig. 10 Lamb Wave Dispersion Curves GFRP

Table 1 Material Property of the Test Specimens

Material	Density( Kg /m <sup>3</sup> )	Poisson's ratio	Velocity (m/s)	Instrument	$E = \frac{V^2 \rho (1 + \nu)(1 - 2\nu)}{1 - \nu}$ (GPa)
CFRP	1400	0.09	7479.36		70
GFRP	1850	0.13	4099.64		26

**Table 2 Lamb Wave Dispersion Properties of the Test Specimens**

Material	Fitted peak Frequency (KHz)	Group ( $C_g$ ) Velocity (m/s)	$\Delta t = d_2 - d_1 / C_g$ (sec)	$\delta = 2\pi f_0 \Delta t$
CFRP	306	1024	$0.156 \times 10^{-3}$	0.30026
GFRP	238	820	$0.195 \times 10^{-3}$	0.29163



**Fig.12 Comparison of  $E'$  &  $E''$  for CFRP and GFRP in Frequency Sweep**

**Table 3 Comparison of the results**

Material	$Tan \delta$		
	Present work	Experimental (DMA)	Theoretical
CFRP	0.005240	0.005213	0.005326
GFRP	0.005089	0.005135	0.005233

Dynamic mechanical analysis (DMA) has become more commonly seen in the analytical laboratory as a tool rather than a research curiosity. This technique is still treated with reluctance and unease, probably due to its importation from the field of rheology. Dynamic mechanical properties refer to the response of a material as it is subjected to a periodic force. These properties may be expressed in terms of a dynamic modulus, a dynamic loss modulus, and a mechanical damping term as shown in fig.11 and fig. 12.

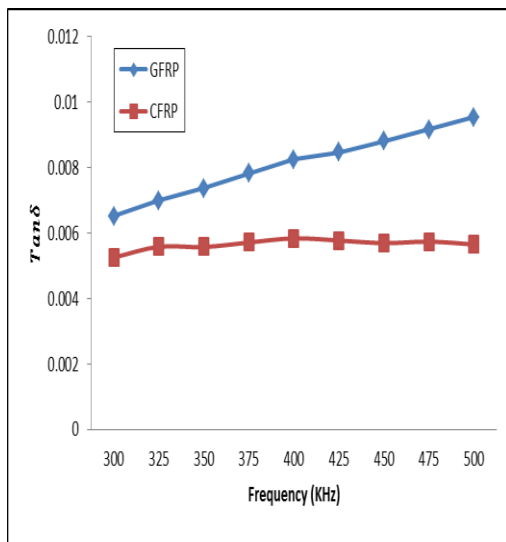


**Fig.11 Comparison of Damping Capacity for CFRP and GFRP in Frequency Sweep**

## VI. CONCLUSION

Vibration damping is the conversion of mechanical vibration energy to thermal energy, and subsequent dissipation of the thermal energy through the volume of the material or structure. Dynamic mechanical analysis is a technique used to study and characterize materials. It is most useful for studying the viscoelastic behavior of polymers. Lamb wave method has been explored in this work and tests were carried out on CFRP and GFRP composite plates. The results of this method were compared with the results of the traditional Dynamic mechanical analyzer (DMA) and they were in close agreement. The main advantage of this method is that the materials can be tested in high frequency range and at relatively low amplitudes and in a non-distractive way.

## REFERENCES

- [1] Y. Chen and R. F. Gibson, "Analytical and Experimental Studies of Composite Isogrid Structures with Integral Passive Damping," *Mechanics of Advanced Materials and Structures*, vol.10(2),pp. 127-143, 2003
- [2] J. Summer scales, *Non-Destructive Testing of Fiber-Reinforced Plastics Composites*, Vol. 1, Elsevier Applied Science, London and New York 1987.
- [3] J.M Berthelot, M. Assarar, Sefrani Y, A.E Mahi, "Damping analysis of composite materials and structures," *Compos. Struct.* vol. 85, pp. 189–204, 2008.
- [4] A. S. Nowick and B. S. Berry, *Anelastic Relaxation in Crystalline Solids*, Academic Press, New York, 1972.
- [5] E.C. Botelho, L.C. Pardini, M.C Rezende, "Damping Behavior of Continuous Fiber/Metal Composite Materials by the Free Vibration Method," *Composites Part B*, vol. 37, pp. 255-264 2006.
- [6] R. F. Gibson, "Nontraditional Applications of Damping Measurements," *STP 1169 Mechanics and Mechanisms of Material Damping*, V. K. Kinra and A. Wolfenden, Editors, 60-75, 1992
- [7] J. Marx, *Rev. Sci. Instrum.* Vol. 22, pp. 503-508, 1951.

- [8] M. R. Harmouche and A. Wolfenden, J. Test Eval., vol. 13, pp. 424-428, 1985.
- [9] G. Gremaud, S.L. Kustov, O. Bremnes, Materials Science Forum, vol. 652, pp. 366-368, 2001.
- [10] H. Guan and R. F. Gibson, "Micromechanical Models for Damping in Woven Fabric-Reinforced Polymer Matrix Composites," Journal of Composite Materials, vol. 35(16), pp. 1417-1434, 2001.
- [11] B. Mu, H.C. Wu, A. Yan, K. Warnemuende, G. Fu, R. F. Gibson and D-W. Kim, "FEA of Complex Bridge System with FRP Composite Deck," Journal of Composites for Construction, vol. 10(1), pp. 79-86, 2006
- [12] A.E Mahi, M Assarar, Y Sefrani, J.M Berthelot, "Damping analysis of orthotropic composite materials and laminates," Composites Part B, vol. 39, pp. 1069-1076, 2008.
- [13] R.P Dalton, P Cawley, and M.J.S. Lowe. "The Potential of Guided Waves for Monitoring Large Areas of Metallic Aircraft Fuselage Structure," Journal of Nondestructive Evaluation, vol.20, pp. 29-46, 2001.
- [14] E.A Birt, "Damage Detection in Carbon-Fibre Composites using ultrasonic Lamb Waves," Insight: Non-Destructive Testing and Condition Monitoring, vol.40, pp 335-339, 1998.
- [15] C. Ratnam, B.S Ben, and B.A Ben, "Structural damage detection using combined finite element and model Lamb wave propagation parameters," IMECHE Part C: Journal of Mechanical Engineering Science, vol. 223, pp. 769-777, 2009.
- [16] P. McIntire,(ed.), Nondestructive Testing Handbook, American Society for Nondestructive Testing, vol.7, pp 398-402, 1991.
- [17] J. Krautkramer, and H. Krautkramer, Ultrasonic Testing of Materials, Berlin, Heidelberg, New York vol.3, pp 580-587, 1983.

#### AUTHOR'S PROFILE

**Mr. B. Avinash Ben**, Dept. of mechanical engg. Andhra University college of engineering (AUCE), Andhra University, Visakhapatnam 530003, India.

**Dr. B. Satish Ben**, Institute of mechanical engg. and technology (IMET), Kyungpook National University, Daegu 702-701, Korea.

**Mr. K. Adarsha Kumar**, Dept. of mechanical engg., GITAM University, Visakhapatnam 530045, India.

**Dr. BSN Murthy**, Dept. of mechanical engg., GITAM University, Visakhapatnam 530045, India.